Metal–Ligand Exchange Coupling in Transition-Metal Complexes

MARSHALL G. CORY and MICHAEL C. ZERNER*

Quantum Theory Project, Department of Chemistry, University of Florida, Gainesville, Florida 32611

Received December 14, 1990 (Revised Manuscript Received April 9, 1991)

Contents

I. Introduction

The electronic spectroscopy of transition-metal complexes is particularly rich due to the three basic types of transitions that can take place. The first of these is localized to the ligand alone, L → L*, and generally resembles that of the ligand, perhaps inductively shifted in frequency. In addition, transitions that are formally forbidden in the ligand may be allowed due to complexation and a lower local symmetry. The second type of transition involves the metal ion alone, and are generally d → d*. These excitations are forbidden in the atom or ion either on spacial symmetry grounds, gerade-to-gerade, "Laporte forbidden",[1,2] or for reasons of spin symmetry. In the former case such transitions gain intensity either through the reduced symmetry of the complex and covalent mixing with the ligand orbitals, or through borrowing, which in turn reduces the symmetry. In the latter case intensity is gained principally through spin–orbit coupling between states of different multiplicities.[3,4]

The third type of transition is ligand to metal L → M* or metal to ligand M → L* charge-transfer excitations.[2] Low-lying excitations of this type generally follow a predictable trend: from easily oxidized ligands to highly oxidized metal ions or from easily oxidized metal ions to easily reduced ligands. Charge-transfer excitations, if they are symmetry and spin allowed, are generally stronger than d → d* but weaker than allowed L → L*. The reason for this is that the transition strength reduces to a calculation of the transition dipole between two orbitals, one of d type and one of ligand type. In the absence of any "covalent" mixing of the d orbitals with ligand orbitals only two center dipole integrals remain, and they are small. Covalency generally increases the transition strength considerably.

These three types of transitions are depicted in Figure 1. This clean distinction into *types* is, of course, destroyed in the presence of strong covalent bonding. The simplicity and regularity just described must be replaced by thinking of the entire complex as a "supermolecule". Symmetry can, however, still be used to yield insight into the physical meaning (if any) of the transition.

Marshall Cory was born in 1951 in Miami, FL. He received his B.Sc. from Florida International University in 1981. He is currently a member of Prof. M. Zerner's research group at the University of Florida. His Ph.D. research includes the theoretical studies of electron–electron and electron–nuclear spin–spin interactions, as well as the investigation of semiempirical descriptions of the spin–orbit interaction as it pertains to calculated electronic spectra.

Michael Zerner was born in 1940 in Boston, MA. He received his B.Sc. at Carnegie-Mellon University in 1961 and his A.M. (1962) and Ph.D. (1968) at Harvard University (Professor Martin Gouterman). He served to the rank of captain in the United States Army and then was an NIH postdoctoral fellow at Uppsala University Sweden, with Per-Olov Lowdin. He is presently a professor of Chemistry and Physics and Chair of Chemistry at the University of Florida. His main scientific interests include electronic structure theories, theories of bonding and reactivity, and electronic spectroscopy.

There is another consideration that can confuse, somewhat, the picture just presented, although in this case the perturbation that complicates this situation might be quite weak leading to results still easily interpretable. This involves spin coupling of the L → L* transitions of different multiplicities with open-shell transition-metal ions. These ligand excitations, normally spin-forbidden, may become allowed. Such

0009-2665/91/0791-0813$09.50/0

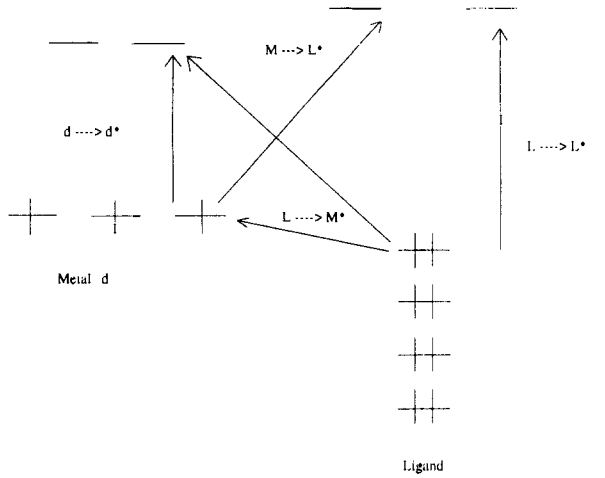

Figure 1. The three basic types of transitions observed in transition-metal complexes: metal to metal (d → d*), ligand to ligand (L → L*), and charge-transfer, ligand to metal (L → M*) and metal to ligand (M → L*).

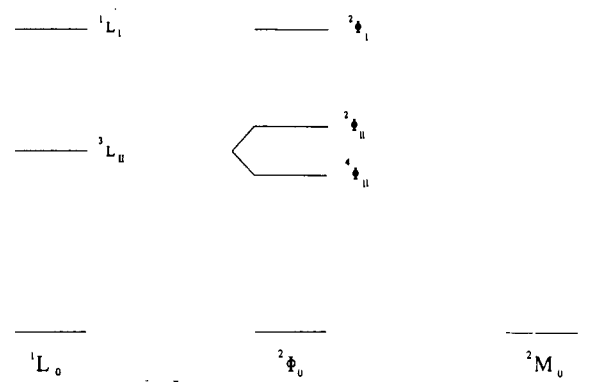

Figure 2. The case of a two open shell transition-metal ion coupling with singlet and triplet ligand states.

transitions are easily mistaken for d → d* or charge transfer. This kind of exchange coupling was examined in detail by Murrell[5] and by Hoijtinck[6] to explain the effect of molecular oxygen on the spectrum of benzene, but is general to any two weakly interacting systems in which at least one such system is paramagnetic. Exchange coupling has been described in some detail for the case of a weakly interacting ligand–transition metal compound in Ake's thesis[7] as well as in a discussion some years ago by Ake and Gouterman.[8,9] With the advent of more accurate self-consistent field–configuration interaction (SCF-CI)[10-17] calculations on excited states, either by ab initio or semiempirical models, it seems desirable to revisit this regularity. The reason for this is that most modern calculations treat the complex as a supermolecule, and this regularity if *not* easily noticed. Worse, most SCF-CI calculations often do not show this regularity, for states of different multiplicities are often biased in energy differently by the SCF procedure itself. For example, (see Figure 2) the quartet and doublets, which result from a triplet L → L* transition exchange coupled to a doublet transition-metal ion, may be at greatly different energies at the molecular orbital level of theory. Often a considerable amount of correlation is required to reestablish the correct parentage of these states and the small splitting that usually characterizes exchange coupling of this type. The reason for this poor initial ordering is that SCF-based methods generally estimate states of higher multiplicity too low in energy relative to states of lower multiplicity. Approximate models that rely heavily on atomic spectroscopy for parameters such as the intermediate neglect of differential overlap/spectroscopic (INDO/S) model,[18-22] often position these transitions correctly even at low levels of configuration interaction (CI). Nevertheless, the hundreds of states that suddenly appear on calculating the excited states of open-shell transition-metal complexes defy easy interpretation without recalling exchange coupling of the kind we describe below.

TABLE I. Summary of Notation

$i,j,k...$	molecular orbitals (ϕ) occupied in the ground state of the ligand
$a,b,c...$	molecular orbitals (ϕ) unoccupied in the ground state of the ligand
$m,n,o...$	metal-based orbitals, in general (d) type
$^{2S+1}L_{(M_s)}$	ligand-based many-electron state of multiplicity 2S + 1
$^{2S+1}M_{(M_s)}$	metal-based many-electron state of multiplicity 2S + 1
$^{2S+1}\Phi_0$	ground state of the complex
$^{2S+1}\Phi_{I,III,V,...,\lambda}$	excited states of the complex with origin stemming from the first, second, ..., $[(\lambda - 1)/2 + 1]$ excited ligand-based singlet state
$^{2S+1}\Phi_{II,IV,VI,...,\lambda}$	excited states of the complex with origin stemming from the first, second, ..., $[\lambda/2]$ excited ligand-based triplet state
$M^{I,II,III,...}$	M designates the metal-based state of highest multiplicity and primes designate states of lower multiplicity (see text under eq 18)

II. Electron–Electron Exchange Coupling

Consider, a ligand state of multiplicity 2s+1 and a metal ion with multiplicity 2s'+1. Then the addition of angular momentum suggests resultant molecular states of $s'' = s + s', s + s' - 1, ..., |s - s'|$, with appropriate multiplicities 2s''+1, etc.[23-25] This implies a direct coupling between the metal and the ligand electronic "spin" systems. The electronic *spin–spin* coupling[26,27] we address in this review arises as a consequence of the antisymmetric nature of electronic wave functions with respect to permutation of electrons. This is all there really is to this subject except for some important subtleties.

Consider the ground state of a ligand as a singlet, $^1L_0$. For simplity let its lowest excited state be dominated by the molecular orbital excitation $\phi_i \rightarrow \phi_a$ (where i,j,k etc. will designate occupied molecular orbitals and a,b,c, etc. unoccupied molecular orbitals, on the ligand). The lowest excited state will then usually be a triplet, viz.

$$^3L_i^a(1) = |\phi_1\bar{\phi}_1...\phi_i\phi_a| \equiv |i\bar{a}|$$

$$^3L_i^a(0) = (1/\sqrt{2})\{|\phi_1\bar{\phi}_1...\phi_i\bar{\phi}_a| - |\phi_1\bar{\phi}_1...\phi_a\bar{\phi}_i|\} \equiv (1/\sqrt{2})\{|i\bar{a}| - |a\bar{i}|\} \quad (1a)$$

$$^3L_i^a(-1) = |\phi_1\bar{\phi}_1...\bar{\phi}_i\bar{\phi}_a| \equiv |\bar{i}\bar{a}|$$

and then followed by the corresponding singlet

$$^1L_i^a(0) = (1/\sqrt{2})\{|i\bar{a}| + |a\bar{i}|\} \quad (1b)$$

where the "bar" over an orbital designates β spin, the values in parentheses are s_z values, and |...| implies the usual Slater determinant.[23,28-31] For ease in the subsequent discussion we summarize our notation in Table I.

Let this ligand now chelate with a doublet metal ion in such a fashion that the overall spin state of the complex is "doublet". The normal spin-allowed transition of the ligand $^1L_0 \rightarrow {}^1L_i^a$ is now more properly described as $^2\Phi_) \rightarrow {}^2\Phi_i^a$ with

$$^2\Phi_0 = \hat{A}[^1L_0{}^1M_0(1/2)] \quad (2a)$$

and

$$^2\Phi_i^a = \hat{A}[^1L_i^a{}^2M_0(1/2)] \quad (2b)$$

where $\hat{A}$ is the antisymmetrizer[31] and $^2M_0(1/2)$ represents the ground-state wave function of the metal. The physics of this situation has not changed; what was formally a singlet-to-singlet transition is now formally a doublet-to-doublet transition.

Let ϕ_m be the singly occupied metal orbital (where m,n,o, etc., are the metal-based d orbitals) that lead to the triplet. The $L \rightarrow L^*$ excitation ($i \rightarrow a$) yields three open-shell orbitals, eight microstates (2^3),[32] one quartet, and two doublets. The construction of the quartet is unique[33]

$$^4\Phi_{II}(3/2) = |iam| = [^3L_i^a(1)^2M_0(1/2)] \quad (3a)$$

Although the two doublets below are not unique, they are constructed to have unique ligand and metal parentage:

$$^2\Phi_I(1/2) = (1/\sqrt{2})\{|\bar{i}am| - |i\bar{a}m|\} = [^1L_i^a(0)^2M_0(1/2)] \quad (3b)$$

$$^2\Phi'_{II}(1/2) = (1/\sqrt{6})\{|i\bar{a}m| + |\bar{i}am| - 2|ia\bar{m}|\} = (1/\sqrt{3})[^3L_i^a(0)^2M_0(1/2) - \sqrt{2}\,{}^3L_i^a(1)^2M_0(-1/2)] \quad (3c)$$

The corresponding energies of these states are

$$^4E_{II} = D - K_{ia} - \tilde{K} \quad (4a)$$

$$^2E_I = D + K_{ia} - (1/2)\tilde{K} \quad (4b)$$

$$^2E_{II} = D - K_{ia} + (1/2)\tilde{K} \quad (4c)$$

where D is an energy common to all these states, and

$$\tilde{K} = (K_{im} + K_{am}) \quad (4d)$$

The exchange integral $K_{\sigma\nu}$ is given by

$$K_{\sigma\nu} = \langle\sigma\nu|\nu\sigma\rangle = \int\int d\tau(1)d\tau(2)\phi_\sigma^*(1)\phi_\nu^*(2)(1/r_{12})\phi_\nu(1)\phi_\sigma(2) \quad (4e)$$

$^4\Phi_{II}$, and $^2\Phi_{II}$ stem from the $^3L_i^a$ ligand state, six microstates where there were, before this coupling, but two. Ligand–metal exchange, $\tilde{K}$, is generally small, thus the quartet and doublet are nearly degenerate with an energy of approximately $D - K_{ia}$. These zero-order splittings can be estimated by eqs 4a–d with the quartet lying lower in accord with Hund's rule.

$^2\Phi_I$ is the normally allowed singlet excited state of the ligand (eq 3b) but whereas in the ligand we observed spin-allowed transitions

$$^1L_0 \rightarrow {}^1L_i^a \leftrightarrow {}^2\Phi_0 \rightarrow {}^2\Phi_I \quad (5a)$$

we also now can observe

$$^1L_0 \rightarrow {}^3L_i^a \leftrightarrow {}^2\Phi_0 \rightarrow {}^2\Phi_{II} \quad (5b)$$

where $^2\Phi_0$ represents the ground-state complex. The number of spin-allowed $L \rightarrow L^*$ excitations has doubled with formally excited state ligand triplets now becoming allowed.

TABLE II. The Coupling of a One Open Shell Metal Ion with Ligand Singlet and Triplet Excited States

quartet

$^4\Phi_{II}(3/2) = |iam| = {}^3L(1)^2M(1/2)$

$^4\Phi_{II}(1/2) = (1/\sqrt{3})\{|i\bar{a}m| + |\bar{i}am| + |ia\bar{m}|\} = (1/\sqrt{3})\{\sqrt{2}\,{}^3L(0)^2M(1/2) + {}^3L(1)^2M(-1/2)\}$

$^4\Phi_{II}(-1/2) = (1/\sqrt{3})\{|i\bar{a}\bar{m}| + |\bar{i}a\bar{m}| + |\bar{i}\bar{a}m|\} = (1/\sqrt{3})\{\sqrt{2}\,{}^3L(0)^2M(-1/2) + {}^3L(-1)^2M(1/2)\}$

$^4\Phi_{II}(-3/2) = |\bar{i}\bar{a}\bar{m}| = {}^3L(-1)^2M(-1/2)$

doublet 1

$^2\Phi_I(1/2) = (1/\sqrt{2})\{|i\bar{a}m| - |\bar{i}am|\} = {}^1L(0)^2M(1/2)$

$^2\Phi_I(-1/2) = (1/\sqrt{2})\{|i\bar{a}\bar{m}| + |\bar{i}a\bar{m}|\} = {}^1L(0)^2M(-1/2)$

doublet 2

$^2\Phi_{II}(1/2) = (1/\sqrt{6})\{|i\bar{a}m| + |\bar{i}am| - 2|ia\bar{m}|\} = (1/\sqrt{3})\{{}^3L(0)^2M(1/2) - \sqrt{2}\,{}^3L(1)^2M(-1/2)\}$

$^2\Phi_{II}(-1/2) = (1/\sqrt{6})\{|i\bar{a}\bar{m}| + |\bar{i}a\bar{m}| - 2|\bar{i}\bar{a}m|\} = (1/\sqrt{3})\{{}^3L(0)^2M(-1/2) - \sqrt{2}\,{}^3L(-1)^2M(1/2)\}$

energy

$E[^4\Phi_{II}(3/2)] = D - K_{ia} - (K_{im} + K_{am})$

$E[^2\Phi_I(1/2)] = D + K_{ia} - (1/2)(K_{im} + K_{am})$

$E[^2\Phi_{II}(1/2)] = D - K_{ia} + (1/2)(K_{im} + K_{am})$

The simple case of a metal-doublet coupling with ligand singlets and triplets is shown in Figure 2 and tabulated in Table II. The normal transition of the spin-forbidden excitation from ground state to triplet (before configuration interactions, CI) is given by

$$E[^3L_i^a] - E[^1L_0] = \epsilon_a - \epsilon_i - J_{ia} \quad (6)$$

In the case of a doublet metal ion this single band is split into two, separated by $(3/2)(K_{im} + K_{am})$ with $^2\Phi_0 \rightarrow {}^2\Phi_{II}$ now spin allowed. In addition to the splitting, the excitations are shifted by an amount equal to $(J_{am} - J_{im}) - (1/4)K_{am} + (3/4)K_{im}$:

$$E[^4\Phi_{II}] - E[^2\Phi_0] = \epsilon_a - \epsilon_i - J_{ia} - (J_{im} - J_{am}) - K_{am} \quad (7a)$$

$$E[^2\Phi_{II}] - E[^2\Phi_0] = \epsilon_a - \epsilon_i - J_{ia} - (J_{im} - J_{am}) + (1/2)K_{am} + (3/2)K_{im} \quad (7b)$$

Similarly, the energy for the normal singlet excitation $^1L_0 \rightarrow {}^1L_i^a$ given by (again in the absence of CI)

$$E[^1L_i^a] - E[^1L_0] = \epsilon_a - \epsilon_i - J_{ia} + 2K_{ia} \quad (8)$$

is shifted and becomes

$$E[^2\Phi_I] - E[^2\Phi_0] = \epsilon_a - \epsilon_i - J_{ia} + 2K_{ia} - (J_{im} - J_{am}) - (1/2)(K_{am} - K_{im}) \quad (9)$$

In the above ϵ_a and ϵ_i are the molecular orbital eigenvalues for the unperturbed ligand and J_{ia} is the Coulomb repulsion integral

$$J_{ia} = \langle ia|ia\rangle = \int\int d\tau(1)d\tau(2)\phi_i^*(1)\phi_a^*(2)(1/r_{12})\phi_i(1)\phi_a(2) \quad (10)$$

Equations such as 7 and 9 are correct only to first order. Major deviations result from configuration mixing among excitations $\Phi_i \rightarrow \Phi_a$ and $\Phi_j \rightarrow \Phi_b$, etc.[22,34] and inductive effects that might raise or lower the eigenvalues of ϵ_a and ϵ_i which are principally ligand in nature. Even so, in the *absence* of covalency (the mixing of d orbitals with ligand orbitals), $\epsilon_i - \epsilon_a$ should remain

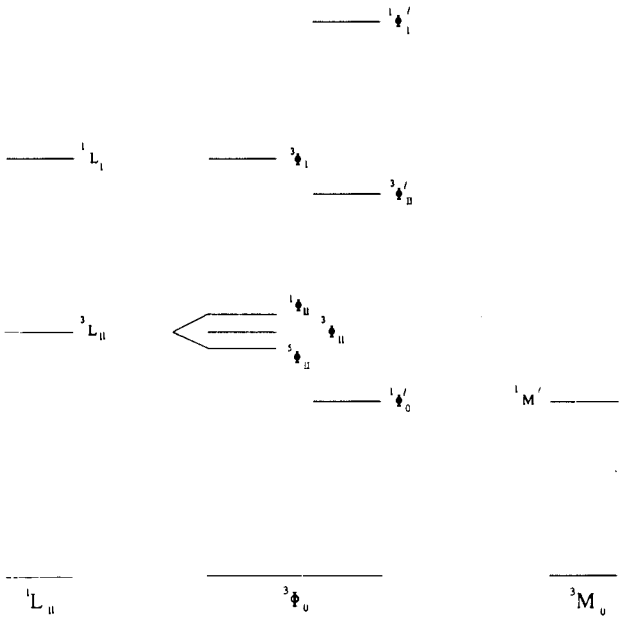

Figure 3. The case of a one open shell transition-metal ion coupling with singlet and triplet ligand states.

TABLE III. The Coupling of a Two Open Shell Metal Ion with Ligand Singlet and Triplet Excited States

quintet

$^5\Phi_{II}(2) = |iamn| = {}^3L(1){}^3M(1)$

triplets

$^3\Phi_I(1) = (1/\sqrt{2})\{|\bar{i}amn| - |i\bar{a}mn|\} = {}^1L(0){}^3M(1)$

$^3\Phi'_{II}(1) = (1/\sqrt{2})\{|ia\bar{m}n| - |iam\bar{n}|\} = {}^3L(1){}^1M'(0)$

$^3\Phi_{II}(1) = (1/2)\{|\bar{i}amn| + |i\bar{a}mn| - |ia\bar{m}n| - |iam\bar{n}|\} = (1/\sqrt{2})\{{}^3L(0){}^3M(1) - {}^3L(1){}^3M(0)\}$

singlets

$^1\Phi'_I(0) = (1/2)\{|\bar{i}a\bar{m}n| - |\bar{i}am\bar{n}| - |i\bar{a}\bar{m}n| + |i\bar{a}m\bar{n}|\} = {}^1L(0){}^1M'(0)$

$^1\Phi_{II}(0) = (1/2\sqrt{3})\{2|\bar{i}\bar{a}mn| + 2|ia\bar{m}\bar{n}| - |\bar{i}a\bar{m}n| - |\bar{i}am\bar{n}| - |i\bar{a}\bar{m}n| - |i\bar{a}m\bar{n}|\} = (1/\sqrt{3})\{{}^3L(-1){}^3M(1) + {}^3L(1){}^3M(-1) - {}^3L(0){}^3M(0)\}$

energy

$E[^5\Phi_{II}(2)] = D - K_{ia} - \bar{K} - (K_{iM} + K_{aM})$

$E[^3\Phi_I(1)] = D + K_{ia} - \bar{K} - (1/2)(K_{iM} + K_{aM})$

$E[^3\Phi'_{II}(1)] = D - K_{ia} + \bar{K} - (1/2)(K_{iM} + K_{aM})$

$E[^3\Phi_{II}(1)] = D - K_{ia} - \bar{K}$

$E[^1\Phi'_I(0)] = D + K_{ia} + \bar{K} - (1/2)(K_{iM} + K_{aM})$

$E[^1\Phi_{II}(0)] = D - K_{ia} - \bar{K} + (1/2)(K_{iM} + K_{aM})$

constant. The shifts given in eqs 7 and 9 are expected to be small, as $J_{im} \simeq J_{am}$ and both K_{am} and K_{im} are, themselves, small.

The case of a triplet metal ion is summarized in Figure 3 and Table III. The three terms arising from the $^3L_{II}$ ($^5\Phi_{II}$, $^3\Phi_{II}$, and $^1\Phi_{II}$) are split by $(3/2)\bar{K} = (3/2)(K_{im} + K_{in} + K_{am} + K_{an})$. In this case, the *newly* allowed transition, $^3\Phi_0 \rightarrow {}^3\Phi_{II}$, has a transition energy given by

$$E[^3\Phi_{II}] - E[^3\Phi_0] = \epsilon_a - \epsilon_i - J_{ia} + (J_{am} + J_{an} - J_{im} - J_{in}) + K_{im} + K_{in} \quad (11)$$

The $^1L_0 \rightarrow {}^1L_I$ singlet becomes $^3\Phi_0 \rightarrow {}^3\Phi_I$ with excitation energy

$$E[^3\Phi_I] - E[^3\Phi_0] = \epsilon_a - \epsilon_i - J_{ia} + 2K_{ia} + (J_{am} + J_{an} - J_{im} - J_{in}) - 1/2(K_{am} + K_{an} - K_{im} - K_{in}) \quad (12)$$

The state $^3\Phi'_{II}$ of Figure 3 is also spin allowed, but should lie considerably higher in energy, as this state represents the coupling of the singlet state of the metal, "spin flip", with the triplet ligand state. The position of $^1M'$ in this diagram is arbitrary, and the position of states $^1\Phi'_0$, $^3\Phi'_{II}$, and $^1\Phi'_I$ will shift up or down accordingly.

Figure 4 shows the case for a three open shell metal (quartet). Where the ligand initially showed one spin-allowed excitation, from the orbital excitation $\phi_i \rightarrow \phi_a$, there are now four. This situation is summarized in

TABLE IV. The Coupling of a Three Open Shell Metal Ion with Ligand Singlet and Triplet Excited States

sextet

$^6\Phi_{II}(5/2) = |iamnp| = {}^3L(1){}^4M(3/2)$

quartets

$^4\Phi_{II}(3/2) = (1/\sqrt{30})\{3|\bar{i}amnp| + 3|i\bar{a}mnp| - 2|ia\bar{m}np| - 2|iam\bar{n}p| - 2|iamn\bar{p}|\} = (1/\sqrt{30})\{3\sqrt{2}\,{}^3L(0){}^4M(3/2) - 2\sqrt{3}\,{}^3L(1){}^4M(1/2)\}$

$^4\Phi'_{II}(3/2) = (1/\sqrt{2})\{|ia\bar{m}np| - |iam\bar{n}p|\} = {}^3L(1){}^2M'(1/2)$

$^4\Phi''_{II}(3/2) = (1/\sqrt{6})\{|ia\bar{m}np| + |iam\bar{n}p| - 2|iamn\bar{p}|\} = {}^3L(1){}^2M''(1/2)$

$^4\Phi_I(3/2) = (1/\sqrt{2})\{|i\bar{a}mnp| - |\bar{i}amnp|\} = {}^1L(0){}^4M(3/2)$

doublets

$^2\Phi_{II}(1/2) = (1/3\sqrt{2})\{|i\bar{a}\bar{m}np| + |i\bar{a}m\bar{n}p| + |i\bar{a}mn\bar{p}| + |\bar{i}a\bar{m}np| + |\bar{i}am\bar{n}p| + |\bar{i}amn\bar{p}| - |ia\bar{m}\bar{n}p| - |ia\bar{m}n\bar{p}| - |iam\bar{n}\bar{p}| - 3|\bar{i}\bar{a}mnp|\} = (1/\sqrt{6})\{\sqrt{2}\,{}^3L(0){}^4M(1/2) - {}^3L(1){}^4M(-1/2) - \sqrt{3}\,{}^3L(-1){}^4M(3/2)\}$

$^2\Phi'_{II}(1/2) = (1/2\sqrt{3})\{|\bar{i}a\bar{m}np| - |\bar{i}am\bar{n}p| + |i\bar{a}\bar{m}np| - |i\bar{a}m\bar{n}p| - 2|ia\bar{m}n\bar{p}| + 2|iam\bar{n}\bar{p}|\} = (1/\sqrt{3})\{{}^3L(0){}^2M'(1/2) - \sqrt{2}\,{}^3L(1){}^2M'(-1/2)\}$

$^2\Phi''_{II}(1/2) = (1/6)\{|\bar{i}a\bar{m}np| + |\bar{i}am\bar{n}p| - 2|\bar{i}amn\bar{p}| + |i\bar{a}\bar{m}np| + |i\bar{a}m\bar{n}p| - 2|i\bar{a}mn\bar{p}| + 2|ia\bar{m}\bar{n}p| + 2|iam\bar{n}\bar{p}| - 4|ia\bar{m}n\bar{p}|\} = (1/\sqrt{3})\{{}^3L(0){}^2M''(1/2) - \sqrt{2}\,{}^3L(1){}^2M''(-1/2)\}$

$^2\Phi'_I(1/2) = (1/2)\{|i\bar{a}\bar{m}np| + |\bar{i}am\bar{n}p| - |i\bar{a}m\bar{n}p| - |\bar{i}a\bar{m}np|\} = {}^1L(0){}^2M'(1/2)$

$^2\Phi''_I(1/2) = (1/2\sqrt{3})\{|i\bar{a}m\bar{n}p| + |i\bar{a}\bar{m}np| - |\bar{i}am\bar{n}p| - |\bar{i}a\bar{m}np| - 2|i\bar{a}mn\bar{p}| + 2|\bar{i}amn\bar{p}|\} = {}^1L(0){}^2M''(1/2)$

energy

$E[^6\Phi_{II}(5/2)] = D - K_{ia} - 3\bar{K} - (K_{iM} + K_{aM})$

$E[^4\Phi_{II}(3/2)] = D - K_{ia} - 3\bar{K} - (1/6)(K_{iM} + K_{aM})$

$E[^4\Phi'_{II}(3/2)] = D - (1/2)(K_{im} + K_{in} + 2K_{ip} + K_{am} + K_{an} + 2K_{ap}) + (1/2)(2K_{mn} - K_{mp} - K_{np})$

$E[^4\Phi''_{II}(3/2)] = D - K_{ia} - (1/6)(5K_{im} + 5K_{in} + 2K_{ip} + 5K_{am} + 5K_{an} + 2K_{ap}) - (1/2)(2K_{mn} - K_{mp} - K_{np})$

$E[^4\Phi_I(3/2)] = D + K_{ia} - 3\bar{K} - (1/2)(K_{iM} + K_{aM})$

$E[^2\Phi_{II}(1/2)] = D - K_{ia} - 3\bar{K} + (1/3)(K_{iM} + K_{aM})$

$E[^2\Phi'_{II}(1/2)] = D - K_{ia} - (1/2)(K_{im} + K_{in} - K_{ip} + K_{am} + K_{an} - K_{ap}) + (1/2)(2K_{mn} - K_{mp} - K_{np})$

$E[^2\Phi''_{II}(1/2)] = D - K_{ia} + (1/6)(K_{im} + K_{in} - 5K_{ip} + K_{am} + K_{an} - 5K_{ap}) - (1/2)(2K_{mn} - K_{mp} - K_{np})$

$E[^2\Phi'_I(1/2)] = D + K_{ia} - (1/2)(K_{iM} + K_{aM}) + (1/2)(2K_{mn} - K_{mp} - K_{np})$

$E[^2\Phi''_I(1/2)] = D + K_{ia} - (1/2)(K_{iM} + K_{aM}) - (1/2)(2K_{mn} - K_{mp} - K_{np})$

TABLE V. The Coupling of a Four Open Shell Metal Ion with Ligand Singlet and Triplet Excited States

septet

$^7\Phi_{II}(3) = {}^3L(1){}^5M(2)$

quintets

$^5\Phi_{II}(2) = (1/\sqrt{6})\{2\,{}^3L(0){}^5M(2) - \sqrt{2}\,{}^3L(1){}^5M(1)\}$

$^5\Phi_I(2) = {}^1L(0){}^5M(2)$

triplet

$^3\Phi_{II}(1) = (1/2\sqrt{15})\{6\,{}^3L(-1){}^5M(2) - 3\sqrt{2}\,{}^3L(0){}^5M(1) + 6\,{}^3L(1){}^5M(0)\}$

energy

$E[^7\Phi_{II}(3)] = D - K_{ia} - 6\bar{K} - (K_{iM} + K_{aM})$

$E[^5\Phi_{II}(3)] = D - K_{ia} - 6\bar{K} - (1/4)(K_{iM} + K_{aM})$

$E[^5\Phi_I(3)] = D + K_{ia} - 6\bar{K} - (1/2)(K_{iM} + K_{aM})$

$E[^3\Phi_{II}(3)] = D - K_{ia} - 6\bar{K} + (1/4)(K_{iM} + K_{aM})$

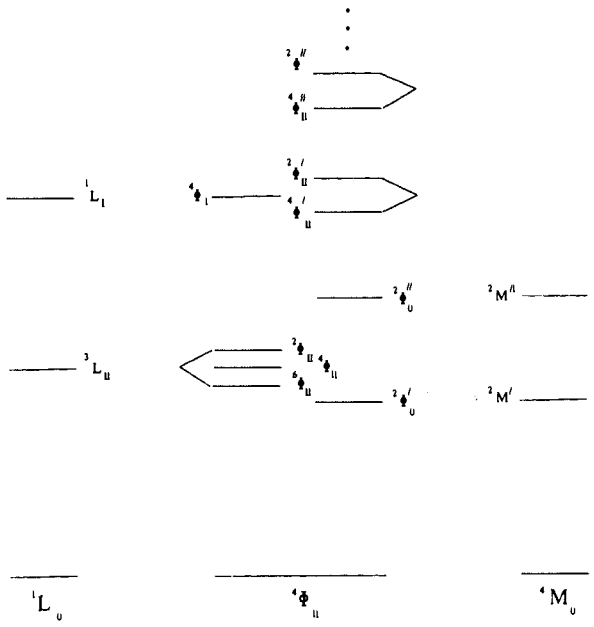

Figure 4. The case of a three open shell transition-metal ion coupling with singlet and triplet ligand states.

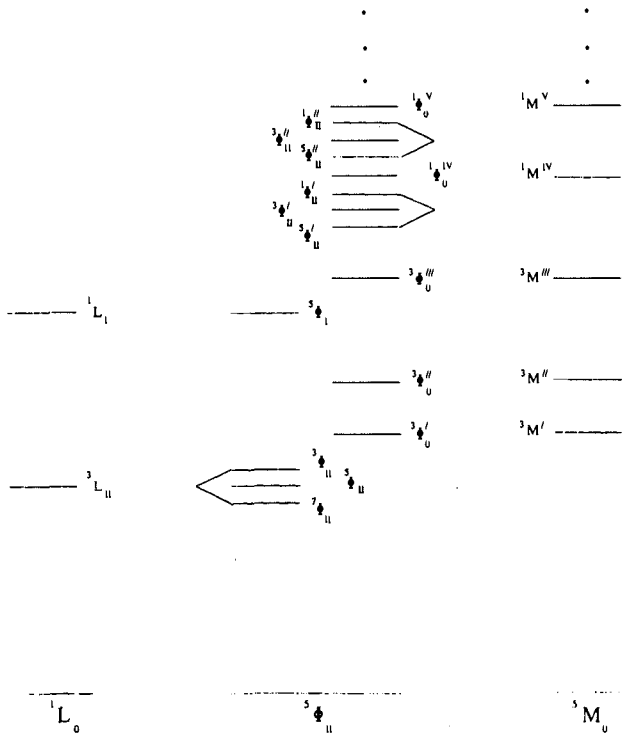

Figure 5. The case of a four open shell transition-metal ion coupling with singlet and triplet ligand states.

Table IV. Tables V and VI summarize the case of the coupling between the ligand and four open shell and five open shell transition metals, respectively. These tables are not complete in that four open shells can generate a quintet, three triplets, and two singlets. Only the coupling to the quintet is given. Similarly five open shells generate a sextet, four quintets and six doublets. Only the coupling to the sextet is given. These *spin-flipped* ($^{2S_m-1}M'$, $^{2S_m-1}M''$, etc.)[33] states lie higher in energy than the state of maximum multiplicity for a given open-shell structure (Hund's rule). Figures 5 and 6 show the situations for a quintet and sextet transition-metal ion, respectively.

TABLE VI. The Coupling of a Five Open Shell Metal Ion with Ligand Singlet and Triplet Excited States

octet

$$^8\Phi_{II}(7/2) = {}^3L(1)^6M(5/2)$$

sextet

$$^6\Phi_{II}(5/2) = (1/\sqrt{7})\{\sqrt{2}\,{}^3L(1)^6M(3/2) - \sqrt{5}\,{}^3L(0)^6M(5/2)\}$$
$$^6\Phi_{I}(5/2) = {}^1L(0)^6M(5/2)$$

quartet

$$^4\Phi_{II}(3/2) = (1/\sqrt{15})\{{}^3L(1)^6M(1/2) - 2\,{}^3L(0)^6M(3/2) + \sqrt{10}\,{}^3L(-1)^6M(5/2)\}$$

energy

$$E[^8\Phi_{II}(7/2)] = D - K_{ia} - 10\bar{K} - (K_{iM} + K_{aM})$$
$$E[^6\Phi_{II}(5/2)] = D - K_{ia} - 10\bar{K} - (5/14)(K_{iM} + K_{aM})$$
$$E[^6\Phi_{I}(5/2)] = D + K_{ia} - 10\bar{K} - (1/2)(K_{iM} + K_{aM})$$
$$E[^4\Phi_{II}(3/2)] = D - K_{ia} - 10\bar{K} + (1/5)(K_{iM} + K_{aM})$$

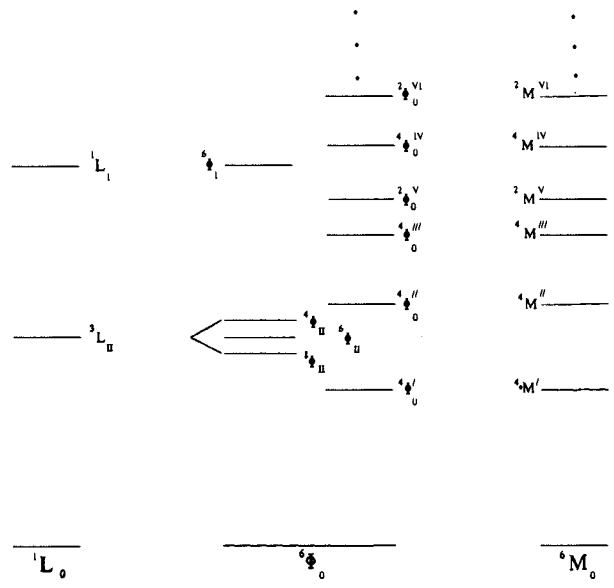

Figure 6. The case of a five open shell transition-metal ion coupling with singlet and triplet ligand states.

Generally, the triplet ligand $^3L_{II}$ state splits into a high multiplicity component with energy given by

$$E[^{2S_m+3}\Phi_{II}(^3L_{II}{}^{2S_m+1}M)] = D - K_{ia} - S_m(2S_m - 1)\bar{K} - (K_{iM} + K_{aM}) \quad (13)$$

and a lowest multiplicity component with energy given by

$$E[^{|2S_m-1|+1}\Phi_{II}(^3L_{II}{}^{2S_m+1}M)] = D - K_{ia} - S_m(2S_m - 1)\bar{K} + (1/2S_m)(K_{iM} + K_{aM}) \quad (14)$$

with a split of

$$\text{split} = (1 + (1/2S_m))(K_{iM} + K_{aM}) \quad (15)$$

The singlet ligand energy is given by

$$E[^{2S_m+1}\Phi_{I}(^1L_{I}{}^{2S_m+1}M)] = D + K_{ia} - S_m(2S_m - 1)\bar{K} - (1/2)(K_{iM} + K_{aM}) \quad (16)$$

with

$$\bar{K} \equiv [1/S_m(2S_m-1)] \sum_{m<n}^{\text{d orbitals}} K_{mn} \quad (17a)$$

$$K_{iM} \equiv \sum_{l}^{\text{d orbitals}} K_{il} \quad (17b)$$

$$K_{aM} \equiv \sum_{l}^{\text{d orbitals}} K_{al} \quad (17c)$$

$$\tilde{K} \equiv K_{iM} + K_{aM} \quad (17d)$$

A d^1 transition-metal ion will possess a manifold of states as shown in Figure 2. Permutations of one electron within the d orbital manifold will not only give rise to d → d* states, but also a superposition of ligand perturbed states, each of which will appear as those in Figure 2. One such excited d → d* is superimposed on another in Figure 7. Recall that all states labeled as doublets are spin allowed. The excitations $^2\Phi_0 \rightarrow {}^2\Phi_0$-(dd*) is the usual d → d* but this excitation also generates a doubling of accessible L → L* states.

The situation is clearly more complex for d^2 metal ions (Figure 3). Here there are 10 possible triplet states, *each* giving rise to a diagram such as that shown in Figure 3. In addition, there are five singlets corresponding to those cases (higher energy) in which the d electrons are paired. The case of three unpaired electrons, d^3, gives rise not only to a superposition of 10 such manifold of states such as those given in Figure 4, but also 20 such diagrams as in Figure 2 corresponding to situations in which two of the d electrons are paired. In spite of these complexities, it is clear that we can describe the excited state manifolds in terms of superposition figures such as those we have given in Figures 2–6.

In order to clarify the origin of these excitations, Ake and Gouterman[7-9] introduced a notation that specified the ligand–metal origin of such states. For example, in Figure 5, the first excited states $^7\Phi_{II}$, $^5\Phi_{II}$, and $^3\Phi_{II}$ are trip-quintets, $^3\Phi'_0$, $^3\Phi''_0$ sing-triplets, and $^5\Phi_I$ a sing-quintet. We have adopted the notation

$$^{2S+1}\Phi^{\mu}_{\lambda} \tag{18}$$

with 2S + 1 the actual multiplicity of the state, λ = 0, I, II for the ground state, the lowest singlet excited L → L* state, and the lowest triplet excited state associated with λ = I (see Table I). λ = III would represent the next highest L → L* singlet, and λ = IV, the triplet associated with it. The superscript μ = 0, ′, ″, ‴, etc. accounts for the metal states of highest multiplicity, S_m, then all those of next highest, S_m–1, then those of S_m–2, in order. [E.g. $^5M \Rightarrow {}^5M(S_z)$, $^3M'(S_z)$, $^3M''(S_z)$, $^3M'''(S_z)$, $^1M^{IV}(S_z)$, and $^1M^{V}(S_z)$, see Figure 6.]

III. Transition Probability

The electronic transition probability between two states can be given in the dipole approximation as an *oscillator* strength[35]

$$f_{IJ} = 4.7092 \times 10^{-7}\, \Delta E_{IJ} |\langle \Psi_I | \vec{\mu} | \Psi_J \rangle|^2 \tag{19}$$

where $\Delta E_{IJ} = E_J - E_I$ in centimeter^{-1}, and $\vec{\mu}$, the dipole operator, is given in debye. Again, in the absence of configuration mixing, the transition moment between a closed-shell ground state $^1L_0$ and $^1L_i^a(0)$ is given by (see eq 1b)

$$\langle {}^1L_0 | \vec{\mu} | {}^1L_i^a(0) \rangle = \sqrt{2} \langle i | \vec{\mu} | a \rangle \tag{20a}$$

or the simple evaluation of the dipole operator between molecular orbitals ϕ_i and ϕ_a. The $^1L_0 \rightarrow {}^3L_i^a$ excitations, are, of course, spin-forbidden

$$\langle {}^1L_0 | \vec{\mu} | {}^3L_i^a \rangle = 0 \tag{20b}$$

and this remains so, to first-order, even after the exchange coupling we have discussed. However, the ligand triplet state that spin couples to create a state of the same multiplicity as the ground state, the trip-"$2S_m$+1 tet", $^{2S_m+1}\Phi_{II}$, $^{2S_m+1}\Phi_{II}$, now mix with the corresponding sing-"$2S_m$+1 tet", $^{2S_m+1}\Phi_I$, and borrow intensity from it.

We examine this for the case of the open-shell metal doublet (Table II) and derive

$$\langle {}^2\Phi_I(1/2) | \hat{H} | {}^2\Phi_{II}(1/2) \rangle = \left(\sqrt{3}/2\right)(K_{am} - K_{im}) \tag{21a}$$

and estimate from first-order perturbation theory[14]

$$^2\tilde{\Phi}_{II}(1/2) \approx {}^2\Phi_{II}(1/2) + \sqrt{3/2}\frac{(K_{am} - K_{im})}{[2K_{ia} - (K_{am} + K_{im})]} {}^2\Phi_I(1/2) \tag{21b}$$

This yields an estimate of the transition dipole between the ground-state doublet to the trip-doublet of[7-9]

$$\langle {}^2\tilde{\Phi}_{II}(1/2) | \vec{\mu} | {}^2\Phi_0(1/2) \rangle = \sqrt{3/2}\frac{(K_{am} - K_{im})}{2K_{ia} - (K_{am} + K_{im})} \langle i | \vec{\mu} | a \rangle \approx \sqrt{3/2}\frac{(K_{am} - K_{im})}{2K_{ia}} \langle i | \vec{\mu} | a \rangle \tag{21c}$$

The transition probability should be small as both K_{am} and K_{im} are expected to be small in the absence of covalency, but it is non-zero. For completeness we note that the ground state $^2\Phi_0(1/2)$ can also mix with the trip-doublet $^2\Phi_{II}(1/2)$ through the last term in the description of $^2\Phi_{II}(1/2)$, viz. $|ia\bar{m}|$ (Table II). The effect of this so-called "Brillouin theorem violating term"[36,37] on the computed oscillator strength can be shown to be small compared to that included in eq 21c.

Equation 21c can be generalized and yields for the transition dipole for the "forbidden" ligand triplet

$$\langle {}^{2S_m+1}\Phi_0 | \vec{\mu} | {}^{2S_m+1}\Phi_{II} \rangle = \frac{(2S_m + 2)(K_{aM} - K_{iM})}{\sqrt{2(2S_m + 2)!!}\, [2K_{ia} - (K_{aM} + K_{iM})/2S_m]} \langle i | \vec{\mu} | a \rangle \tag{22a}$$

with

$$A!! = (A)(A-2)!! \qquad 1!! = 1 \qquad 2!! = 2 \tag{22b}$$

Before concluding this section it is important to point out that most of the intensity that derived from transitions, from the ground state to excited states, stem from single excitations of the type $\phi_i \rightarrow \phi_a$. This is simply a manifestation of the one-electron nature of the dipole transition operator. Transitions from the ground state to states that are principally double (or higher) excitations can only gain intensity through configurational mixing with single excitations, or through the mixing of the ground state with excited configurations. This observation gives utility to diagrams such as those shown in Figures 2–6. The superposition of such diagrams represented in Figure 7 gives a more complete representation of the available manifold of excited states, but the actual ground state, and the excited states that are principally singly excited relative to this ground-state, will give the major features of this spectrum. In other words, in Figure 7, $^2\Phi_0 \rightarrow {}^2\Phi_0$(dd*) or (d → d*) might be observed, but other $^2\Phi_\lambda$(dd*) will probably not be, as they are doubly (or higher) excited relative to $^2\Phi_0$.

IV. Effects of Covalency

Throughout these discussions we have assumed that the mixing of ligand molecular orbitals and metal or-

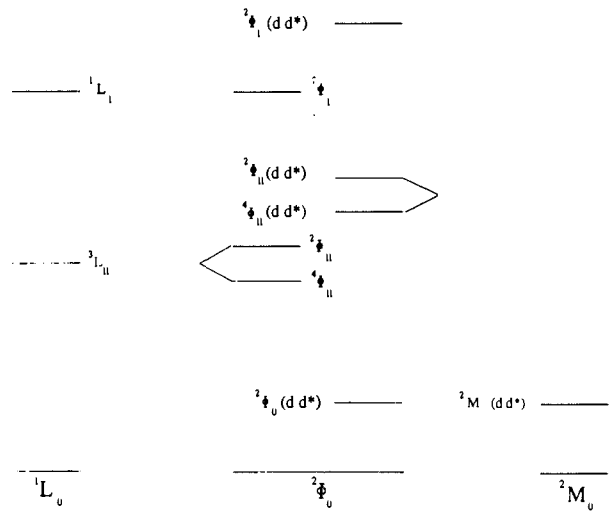

Figure 7. Ligand-based states that are generated through d → d* excitation. States designated $^{2S+1}\Phi_A(dd^*)$, $A \neq 0$, differ from $^2\Phi_0$ by two orbital assignments. See text.

bitals (covalency) is minor, and thus the perturbation of the ligand by the metal is minor and essentially confined to inductive effects and exchange coupling of the type we have discussed here. Regardless, the description of the configuration in terms of determinants that we present in the tables and the energies we assign to these remain valid. The utility of the description of the states in terms of "L" and "M" many-electron functions, however, does degenerate with increasing covalency, as the uniqueness of the choice of states of the same multiplicity stemming from the same electronic configuration becomes less meaningful. For example, the choice of the three triplets of Table III is not unique. The utility of this particular choice rests on the observation that one of these is associated with the ligand singlet, one with the ligand triplet and one with a spin flip on the metal. That is, that these three states do not have large mixing among themselves. This, in turn, depends on the fact that K_{im} and K_{am} are smaller than both K_{ia}, the intraligand exchange, and K_{mn}, the exchange between two d orbitals. Matrix elements between two states of arbitrary ϕ_i, ϕ_a, and ϕ_m take the form of those given in eq 21. We derive, for example, the condition that $(K_{aM} - K_{iM})/2S_m < [2K_{ia} - (K_{aM} + K_{iM})/2S_m]$ for small mixing, between Φ_I and Φ_{II}. Similar expressions compare differences of metal–ligand exchange integrals with $[2\bar{K} - (K_{aM} + K_{iM})/2S_m]$ for determining mixing of spin-flip states with the trip-"-$(2S_m+1)$ tets" of interest. For ϕ_i, ϕ_a, and ϕ_m localized to the ligand and metal respectively, this is clearly the case. This condition also remains intact even for reasonable amounts of covalency (<10–20%) for the correction terms in an analysis of covalency tend to cancel. Beyond this, the approximate breakdown into "L" and "M" many-electron fragments degenerates quickly and only a supermolecule description seems appropriate.

V. Examples

A. Porphinatoiron(III) Chloride

We present, as an example, the calculated spectrum of porphinatoiron(III) chloride, the molecule given in Figure 8.[38-40] This spectrum is somewhat complicated in that it requires, at a minimum, consideration of the

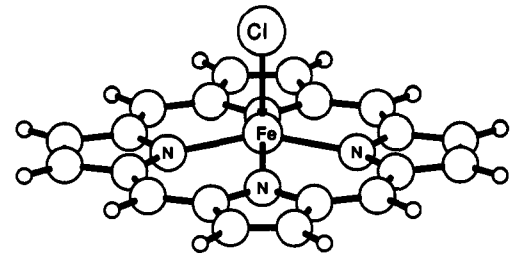

Figure 8. Porphinatoiron(III) chloride.

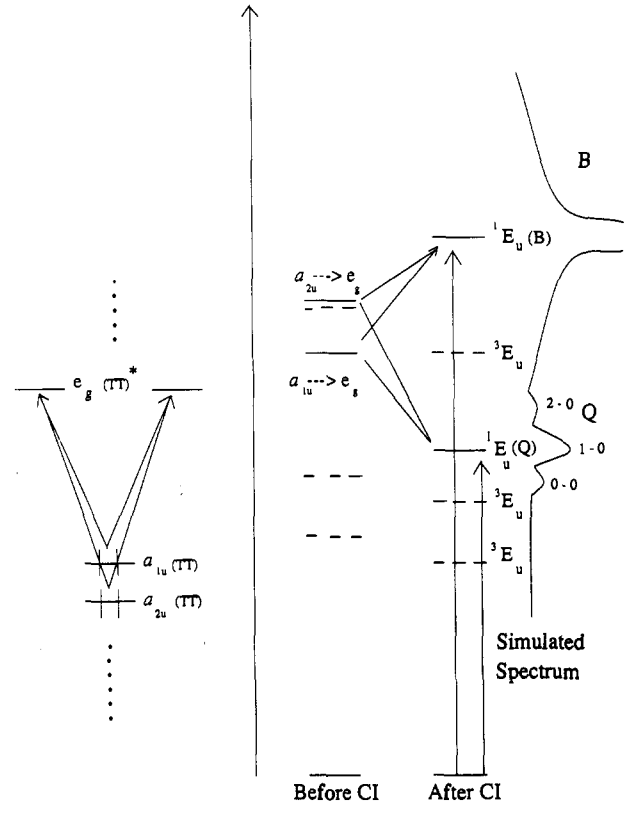

Figure 9. The "four orbital model" description of the spectrum of porphyrin: ---, triplet and —, singlet.

two highest filled porphyrin [$a_{1u}(\pi)$ and $a_{2u}(\pi)$] and the two lowest empty porphyrin [$e_g(\pi^*)$] molecular orbitals, to describe the ligand spectrum, as shown in Figure 9.[40] The results we present are from SCF-CI[10-17] calculations of the INDO/S type.[18-22]

The "B" band, or "Soret" band, is very intense, and we consider here only the calculated states of lower energy. As suggested in Figure 9, the two triplets, the "Q" band, and another triplet with origin outside of the four orbital model,[40] and the "B" band will all contribute to the allowed spectrum in the lower energy region after metal–ligand spin–spin coupling. All of these states are of E_u (E) symmetry.

In Figure 10 we summarize the salient features of the calculated spectrum of this system assuming the ground state is of $^2B_{2g}$ ($^2B_2$) type, and then of ^2E_g (^2E) type.

In the following discussion we will give both D_{4h} labels as is conventional in porphyrin spectroscopy, and the actual C_{4v} symmetry labels in parentheses. The principal intensity will lie in transitions related to the reference through single-excitations as described previously.

Figure 10 also demonstrates another type of important interaction between ligand and metal that is spacial

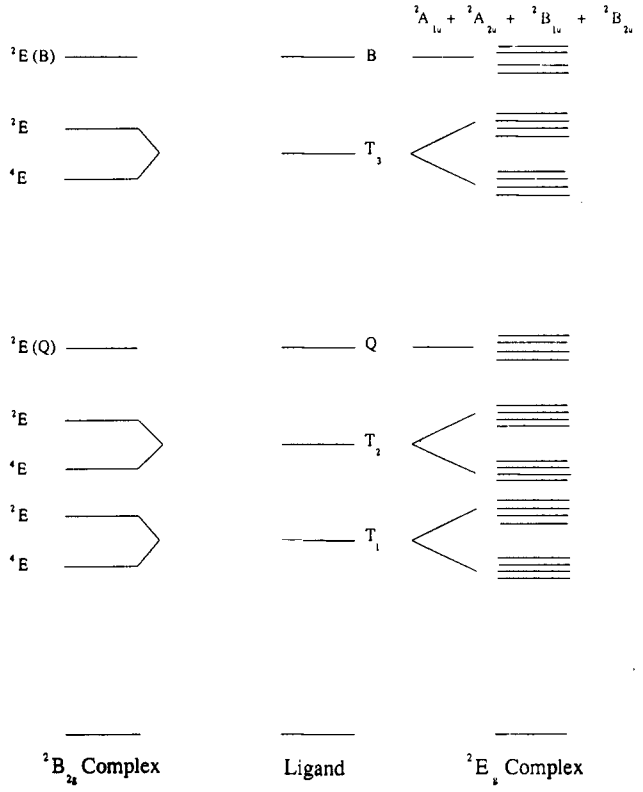

Figure 10. The calculated spectrum of porphinatoiron(III) chloride assuming a $^2B_{2g}$ and ^2E_g ground state.

(rather than spin) in nature. If the metal ion is in a degenerate state before coupling, and the states of interest of the ligand are degenerate, then the direct product representation can cause further splittings. In this case, the ligand triplet and singlet states of interest are of E_u (E) symmetry, coupling with the ^2E_g (^2E) state of the Fe(III) ion. In the D_{4h} point group $E_u \otimes E_g = A_{1u} + A_{2u} + B_{1u} + B_{2u}$ and in the C_{4v} point group $E \otimes E = A_1 + A_2 + B_1 + B_2$.[41] This leads not only to the spin–spin coupling we have been discussing until now, but also to a spacial coupling and resulting splitting of states. In the original ligand, only B and Q bands are allowed. In coupling with the doublet, three trip-doublets below the B band gain intensity and the lowest energy one might be observed in absorption experiments. When the reference is ^2E_g (^2E), 20 separate states below the B band (and including the B band) in energy gain intensity, when only two were allowed in the isolated porphyrin ligand.

The ^2E_g state ($d_{xz}^2 d_{yz} d_{xy}^2$) is believed to be the lowest lying state for ferricytochrome-C[40] and for most metmyoglobins.[43,44] In all cases, the Q band is broadened and appears in the range 16 900–18 900 cm^{-1}. We calculate very many states before the Q band (Table VII) including $d_\pi \rightarrow d_{z^2}$ and $d_{xy} \rightarrow d_{z^2}$ and the charge-transfer states, $a_{1u}(\pi) \rightarrow d_{z^2}$ and $a_{2u}(\pi) \rightarrow d_{z^2}$. The two trip-doublets associated with the lowest porphyrin triplet states are calculated at 10 921–12 883 cm^{-1} and 15 740–17 857 cm^{-1}. The first of these has a calculated oscillator strength of 0.002 and should be observable. The calculated trip-quartets lie about 200 cm^{-1} below their corresponding trip-doublets (Table VII) except for the lowest trip-doublet, which has been depressed through configuration mixing with the sing-doublet and has gained intensity through this mixing (eq 21c). The second group of trip-doublets has a calculated oscillator

TABLE VII. The Calculated Spectrum of Porphinatoiron(III) Chloride Assuming a ^2E_g Ground State (Unless Labeled "Quartet" These States Are All Doublets)

label	calculated ^2E_g excitation energies: type	energy, cm^{-1}	oscillator strength
$d(\pi) \rightarrow d(z^2)$	$^2A_{2g}(dd^*)$	3 014.0	
$d(xy) \rightarrow d(\pi)$	$^2B_{2g}(dd^*)$	3 617.0	
$d(\pi) \rightarrow d(z^2)$	$^2A_{2g}(dd^*)$	6 715.0	
$d(\pi) \rightarrow d(z^2)$	$^2A_{2g}(dd^*)$	7 535.0	
$d(xy) \rightarrow d(z^2)$	$^2E_g(dd^*)$	10 633.0	
T_1	trip-doublet (Q)	10 921.0	0.002
quartet	trip-doublet (Q)	12 607.0	
quartet	trip-doublet (Q)	12 632.0	
quartet	trip-doublet (Q)	12 653.0	
quartet	trip-doublet (Q)	12 700.0	
	trip-doublet (Q)	12 806.0	
	trip-doublet (Q)	12 877.0	
	trip-doublet (Q)	12 883.0	
$a_{1u} \rightarrow d(z^2)$	Tx	13 855.0	
$d(\pi) \rightarrow d(z^2)$	$^2A_{2g}(dd^*)$	14 404.0	
$d(xy) \rightarrow d(z^2)$	$^2E_g(dd^*)$	14 769.0	
T_2	trip-doublet (B)	15 740.0	0.001
$a_{2u} \rightarrow d(z^2)$	Tx	16 041.0	0.001
T_2 quartet	trip-doublet (B)	17 292.0	
quartet	trip-doublet (B)	17 297.0	
quartet	trip-doublet (B)	17 320.0	
quartet	trip-doublet (B)	17 323.0	
	trip-doublet (B)	17 746.0	0.002
	trip-doublet (B)	17 826.0	0.001
	trip-doublet (B)	17 857.0	0.001
Q	sing-doublet	18 456.0	0.081
$a_{1u} \rightarrow d(z^2)$	Tx	18 469.0	
Q	sing-doublet	18 660.0	0.063
	sing-doublet	18 711.0	0.075
Q	sing-doublet	18 731.0	0.074
•	•	•	•
•	•	•	•
•	•	•	•
B	sing-doublet	30 150.0	1.248
	sing-doublet	30 365.0	1.025
	sing-doublet	30 418.0	1.248
	sing-doublet	30 706.0	1.094

strength that sums to 0.004, but would likely be hidden by the Q bands with calculated oscillator strength that totals 0.293. We estimate from SCF-CI calculations on each species separately that the $^2B_{2g}$ ($d_{xz}^2 d_{yz}^2 d_{xy}$) lies 1800 cm^{-1} above the ^2E_g (corresponding to $d_{xy} \rightarrow d_\pi$) and that the $^2A_{2g}$ ($d_{xy}^2 d_{xz} d_{z^2}$) state lies 2100 cm^{-1} above the ^2E_g (corresponding to the $d_\pi \rightarrow d_{z^2}$ excitation). A measure of the consistency of this procedure is obtained by comparing these values with those calculated from the CI, assuming a ^2E_g reference state. These values appear in Table VII as 3600 and 3000 cm^{-1}, which shows a reveral in the order of states, but an average "error" of only 1300 cm^{-1}.

If the calculated spectrum, assuming ground states of ^2E_g, $^2B_{2g}$, and $^2A_{2g}$, is of the singles-only type (CIS), as is often the case in semiempirical schemes, a superposition of the calculated manifolds assuming an offset of 1800 cm^{-1} for the $^2B_{2g}$ states and 2100 cm^{-1} for the $^2A_{2g}$ states gives a good feel for the nature of the low-lying states and suggests the regularities that should be apparent in a larger calculation.[45] The spectroscopy of the ^2E_g species, however, will still be dominated by those states that are singly excited relative to the ^2E_g reference.

There are literally thousands of states that are represented, for example, by the superposition of diagrams such as the two given in Figure 10. In general, all the excited states are represented *in principal* by a greater

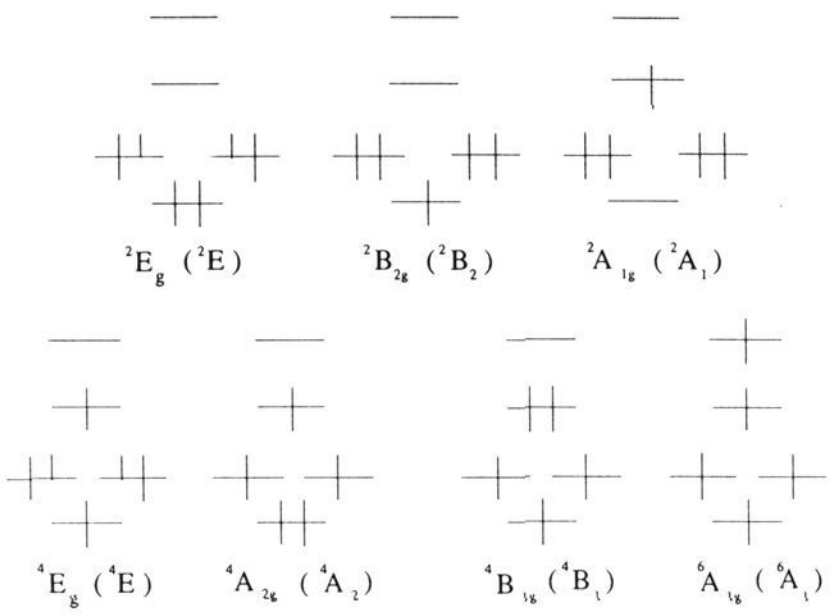

Figure 11. The symmetry of the metal states in a D_{4h} (C_{4v}) field. The half electron in a d_π orbital signifies a wave function of the type $(1/\sqrt{2})(|d_{xz}\overline{d_{xz}}d_{yz}| \pm |d_{yz}\overline{d_{yz}}d_{xz}|)$.

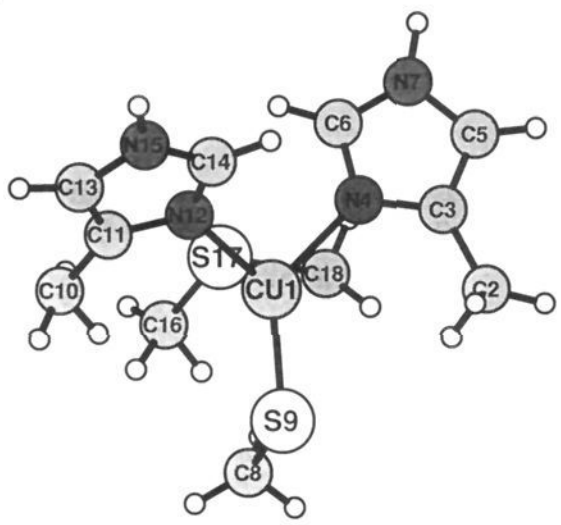

Figure 12. The assumed structure of plastocyanine. See refs 49 and 50.

CI that includes *at least* all single excitations from all the reference states suggested in Figure 11.[46-49] The utility of a superposition of such diagrams as given in Figure 10 rests upon weak coupling between metal and ligand, and the fact that most of the oscillator strength for transitions of a system in a well-characterized ground state results from single excitations from that ground state. Given these caveats a superposition of such diagrams[50] does show the regularities that *should* be apparent in the larger CI.

For completeness, we note tht in the particular case of the model compound porphinatoiron(III) chloride the $^4A_{2g}$ state is believed to lie lowest in energy, with the $^6A_{1g}$ state less than 1000 cm^{-1} above.[39]

B. Plastocyanine

As a second example we present a calculation of the excited states of plastocyanine.[51] The structure adopted is from ref 52 and is given in Figure 12. The calculated spectrum appears in Table VIII, where it is compared with experimental values reported by Solomon, Hare, and Gray.[53] Also reported in Table VIII is the calculated spectrum of the "bare" imidazole and imidazolate complexes of Figure 12 without copper, $(SCH_3)^-$, and $S(CH_3)_2$. The peaks from 6400 to 17 000 cm^{-1} are all associated with excitations into the singly occupied HOMO, an orbital about 67% Cu and 20% of the S of $(SCH_3)^-$. The peak calculated at 17 000 cm^{-1} we associate with the "signature" copper blue line[53] common to the complexes.

TABLE VIII. The Calculated Spectra of Plastocyanine and the Imidazole–Imidazolate Complex (Energies are in Units of $cm^{-1} \times 10^{-3}$, the Calculated Oscillator Strengths Are in Parentheses)

imidazole–imidazolate complex		plastocyanine		
singlet	triplet	observed	calculated[a]	comments[b]
		5.5	6.4 (0.0007)	$(SCH_3)^- \rightarrow$ HOMO
		10.3	8.1[c] (0.0017)	$N_2 \rightarrow$ HOMO
		11.9	9.4[c] (0.0082)	$N_2 \rightarrow$ HOMO
		13.6	11.2 (0.0009)	$N_2 \rightarrow$ HOMO
			11.4[c] (0.0013)	$N_2 \rightarrow$ HOMO
		16.6	17.0 (0.1020)	$N_2 \rightarrow$ HOMO
			[19.3 [Q]	trip-doublets
	16.8	18.1	19.6 (0.0000)]	$N_1 \rightarrow N_1$
			[19.3 [Q]	trip-doublets
	21.9		20.1 (0.0003)]	$N_2 \rightarrow N_2$
		21.5	21.1 (0.0087)	$N_2 \rightarrow$ HOMO
		23.6	22.9 (0.0540)	$N_2 \rightarrow$ HOMO
			[24.8 [Q]	trip-doublets
	26.0		25.3 (0.0025)]	$N_2 \rightarrow N_2$
			[26.3 [Q]	trip-doublets
	27.1		26.6 (0.0000)]	$N_1 \rightarrow N_1$
28.3 (0.0058)			28.9 (0.0062)	sing-doublet $N_2 \rightarrow N_1$
			[28.7 [Q]	trip-doublets
	28.3		29.1 (0.0000)]	$N_2 \rightarrow N_1$

[a] From ref 51. [Q] designates the quartet component. [b] The HOMO is an orbital of about 67% Cu and 20% $(SCH_3)^-$ and is characteristic of the complex. N_1 is imidazole and N_2 imidazolate. [c] The energies of these peaks are reasonably sensitive to the assumed geometry. See Figure 12.

Peaks calculated at 19 600 and 20 100 cm^{-1} are trip-doublets associated with imidazole and imidazolate triplet states as indicated in the table. Similarly peaks calculated at 25 300 and 26 600 cm^{-1} are also associated with imidazole and imidazolate triplets. The peaks calculated at 28 900 and 29 100 cm^{-1} are sing-doublet and trip-doublet states associated with imidazolate–imidazole ($N_2 \rightarrow N_1$) charge-transfer excitations. That they lie within 200 cm^{-1} of each other is a consequence of a very small K_{ia} value between ϕ_i on the imidazolate and ϕ_a on imidazole (Table I). Note for small K_{ia}, the sing-doublet lies below the trip-doublet, as calculated.

Although there is much to say about the chemistry of this system,[51] it is rather interesting that even with the amount of covalency shown in this calculation between Cu and S, the spectrum is easily interpreted in terms of this exchange coupling model.

VI. Conclusion

In this article the effect of ligand–metal electron exchange coupling as it pertains to the calculated electronic spectra of transition-metal complexes has been reviewed. Through the use of example calculations, along with the accompanying tables and figures, the increase in the number of spin-allowed electronic excitations due to this exchange coupling has been delineated. We present closed formulas for the splitting of the multiplets due to this interaction. The predicted intensity of these *newly* spin-allowed excitations was addressed in section III, and we also present closed formulas for this oscillator strength. The calculated spectra of porphinatoiron(III) chloride and plastocyanine were offered as examples in section IV. For the case of porphinatoiron(III) chloride, in addition to the exchange coupling that gives intensity to the lowest

lying porphyrin triplet state, which is well explained in terms of the analysis we present, there is a further splitting of levels due to symmetry. The excited ligand states of interest are ^1E and ^3E, while that of the coupling Fe(III) is ^2E. This spacial coupling splits the dipole-allowed porphyrin E states into B_1, B_2, A_1, and A_2 nondegenerate states. The plastocyanine example demonstrates the applicability of the exchange-coupling model to systems where the assumption of no (or little) covalent mixing is not rigorously obeyed. The Cu–S covalency in the plastocyanine system is sufficiently strong to disrupt the picture of "clean" molecular orbitals. That is, the picture of molecular orbitals localized on the ligand, and molecular orbitals of almost pure metal "d" atomic character, has begun to fail. Even so, the calculated spectrum is still easily interpreted in terms of this model.

As can be seen in Tables VII and VIII, the calculated spectra of transition-metal complexes are rich in structure. With the advent of fast, relatively inexpensive desk top computers, and the availability of sophisticated quantum chemical program packages, such spectra calculations will become routine to both the specialist and nonspecialist. It is our hope that this review will aid in interpreting the results of these calculations, yielding a useful description of the calculated results, and, perhaps, prevent possible misinterpretations due to exchange splittings that are calculated too large relative to experiment, a consequence of an incomplete theoretical treatment. It is also our hope to remind the reader that in addition to the d → d* and charge-transfer excitations that appear in the low energy spectra of transition-metal complexes, weakly allowed formally spin-forbidden L → L* excitations should be observed.

Acknowledgments. This work has been supported in part by grants from the Eastman Kodak Co. and from the Natural Science and Engineering Council of Canada.

References

(1) Levine, I. N. *Molecular Spectroscopy*, John Wiley & Sons: New York, 1975; Chapter 3.
(2) Ballhausen, C. J. *Introduction to Ligand Field Theory*; McGraw-Hill: New York, 1962.
(3) Piepho, S. B.; Schatz, P. N. *Group Theory in Spectroscopy*; John Wiley & Sons: New York, 1983.
(4) Herzberg, G. *Spectra of Diatomic Molecules*; Van Nostrand Reinhold Co.: New York, 1966.
(5) Murrell, J. N. *Mod Phys.* **1960**, *3*, 319.
(6) Hoijtinck, G. J. *Mod Phys.* **1960**, *3*, 67.
(7) Ake, R. L. Ph.D. Thesis Department of Chemistry, Harvard University, 1968.
(8) Ake, R.; Gouterman, M. *Theor. Chim. Acta* **1969**, *15*, 20.
(9) Ake, R.; Gouterman, M. *Theor. Chim. Acta* **1970**, *17*, 408.
(10) Roothan, C. C. J. *Rev. Mod. Phys.* **1951**, *23*, 69.
(11) Roothan, C. C. J. *Rev. Mod. Phys.* **1960**, *32*, 179.
(12) Pople, J. A.; Nesbet, R. K. *J. Chem. Phys.* **1954**, *22*, 571.
(13) Schaefer, H. F., Ed. *Methods of Electronic Structure Theory*; Plenum: New York, 1977; Chapter 4.
(14) Ritz, W. *J. Reine Angew. Math.* **1909**, *135*, 1.
(15) Eckart, C. *Phys. Rev.* **1930**, *36*, 878.
(16) Szabo, A.; Ostlund, N. S. *Modern Quantum Chemistry*; McGraw-Hill: New York, 1989; Chapter 4.
(17) Schaefer, H. F., Ed. *Methods of Electronic Structure Theory*; Plenum: New York, 1977; Chapters 6 and 7.
(18) Pople, J. A.; Beveridge, D. L.; Dobosh, P. *Chem. Phys.* **1967**, *47*, 2026.
(19) Ridley, J. E.; Zerner, M. C. *Theor. Chim. Acta* **1973**, *32*, 111.
(20) Ridley, J. E.; Zerner, M. C. *Theor. Chim. Acta* **1976**, *42*, 223.
(21) Bacon, A. D.; Zerner, M. C. *Theor. Chim. Acta* **1979**, *53*, 21.
(22) Zerner, M. C.; Loew, G. H.; Kirchner, R. F.; Mueller-Westerhoff, U. T. *J. Am. Chem. Soc.* **1980**, *102*, 589.
(23) Szabo, A.; Ostlund, N. S. *Modern Quantum Chemistry*; McGraw-Hill: New York, 1989; Chapter 2.
(24) Merzbacher, E. *Quantum Mechanics*; John Wiley & Sons: New York, 1970; Chapter 9.
(25) Condon, E. U.; Shortley, G. H. *The Theory of Atomic Spectra*; Cambridge: London, 1964; Chapter 3.
(26) Seitz, F. *The Modern Theory of Solids*; McGraw-Hill: New York, 1940; p 612.
(27) Dekker, A. J. *Solid State Physics*; Prentice Hall: New Jersey, 1961; p 472.
(28) Pauncz, R. *Spin eigenfunctions*; Plenum: New York, 1979.
(29) Pauling, L.; Wilson, E. B. *Introduction to Quantum Mechanics*; McGraw-Hill: New York, 1935.
(30) Slater, J. C. *Quantum Theory of Matter*; McGraw-Hill: New York, 1968.
(31) Pople, J. A.; Beveridge, D. L. *Approximate Molecular Orbital Theory*; McGraw-Hill: New York, 1970; p 17.
(32) Pauncz, R. *Spin eigenfunctions*; Plenum: New York, 1979; p 11.
(33) A complete discussion of this notation is given for eq 18.
(34) Parr, R. G. *Quantum Theory of Molecular Electronic Structure*; Benjamin Press: Boston, 1963.
(35) Eyring, H.; Walter, J.; Kimball, G. E. *Quantum Chemistry*; John Wiley & Sons: New York, 1960.
(36) Edwards, W. D.; Zerner, M. C. *Theor. Chim. Acta* **1987**, *72*, 347.
(37) Davidson, E. R. *Chem. Phys. Lett.* **1973**, *21*, 565. Jackels, C. F.; Davidson, E. R. *Int. J. Quantum Chem.* **1974**, *8*, 707.
(38) Edwards, W. D.; Weiner, B.; Zerner, M. C. *J. Am. Chem. Soc.* **1986**, *108*, 2196.
(39) Edwards, W. D.; Weiner, B.; Zerner, M. C. *J. Phys. Chem.* **1988**, *92*, 6188.
(40) Gouterman, M. *J. Mol. Spectrosc.* **1961**, *6*, 138.
(41) See, for example: Cotton, F. A. *Chemical Applications of Group Theory*; John Wiley & Sons: New York, 1990.
(42) Eaton, W. A.; Hochstrasser, R. N. *J. Chem. Phys.* **1967**, *46*, 2533.
(43) Makinen, M. W.; Churg, A. K. In *Iron Porphyrins*; Lever, Gray, Eds.; Addison-Wesley: Boston, MA, 1983; Part 1.
(44) Schejter, A.; Eaton, W. A. *Biochemistry* **1984**, *23*, 1081.
(45) Care must be exercised in such a superposition of diagrams, as an SCF calculation assuming a ground state of $^2B_{2g}$ or $^2A_{2g}$ symmetry is likely to yield the ^2E_g state as excited unless followed by a great deal of CI. This is due the orbital relaxation that prejudicially lowers the energy of the SCF states relative to others. One test of the consistency of the INDO/S procedure has already been given in the text.
(46) In actual applications we would need to include single, double, and triple excitations from each of the reference states suggested in Figure 11, a formidable task for such a large molecule.
(47) Rawlings, D.; Gouterman, M.; Davidson, E. R.; Feller, D. *Int. J. Quantum Chem.* **1985**, *28*, 773.
(48) Rawlings, D.; Gouterman, M.; Davidson, E. R.; Feller, D. *Int. J. Quantum Chem.* **1985**, *28*, 797.
(49) Rawlings, D.; Gouterman, M.; Davidson, E. R.; Feller, D. *Int. J. Quantum Chem.* **1985**, *28*, 823.
(50) Seel also: Konis, E.; Kremer, S. *Ligand Field Energy Diagrams*; Plenum: New York, 1977.
(51) Correa de Mello, P.; Larsson, S.; Zerner, M. Manuscript in preparation.
(52) Guss, J. M.; Freeman, H. C. *J. Mol. Biol.* **1983**, *169*, 521.
(53) Solomon, E. I.; Hare, J. W.; Gray, H. B. *Proc. Natl. Acad. Sci. U.S.A.* **1976**, *73*, 1389.